# QUANTIFYING THE EFFECTS OF AMORPHOUS LAYERS ON IMAGE CONTRAST USING ENERGY FILTERED TRANSMISSION ELECTRON MICROSCOPY

C. B. BOOTHROYD, R. E. DUNIN-BORKOWSKI, W. M. STOBBS AND
C. J. HUMPHREYS
Department of Materials Science and Metallurgy, University of Cambridge, Pembroke Street,
Cambridge, CB2 3QZ, U.K.

## ABSTRACT

High resolution images of a block oxide, $(Nb_2O_5)_9(WO_3)_8$, with and without a superposed carbon film are compared both energy filtered and including the inelastic scattering. The differences between the images are quantified on an absolute intensity scale and possible origins of the differences in atomic level contrast are assessed using multislice simulations.

## INTRODUCTION

If high resolution imaging is to become truly useful in the characterisation of structure then the images obtained need to be fully quantified. While vectorial analysis of the local intensity and contrast in a characteristic area, as well as the Fourier analysis of such templates, facilitates image quantification, it is as yet not widely recognised that matches of such images with the equivalent conventional simulations are generally poor [1], and particularly so when the imaging parameters and the thickness of the specimen are determined by independent means. Part of the problem lies in the contributions to the image detail caused by inelastic scattering [e.g. 2, 3] so that filtered images, now obtainable using both Zeiss filtered microscopes (912) as well as high resolution electron microscopes fitted with added filters such as the Gatan Imaging Filter, allow a major step forward. Nonetheless a further problem derives from the effect of the contamination and damage on a specimen, particularly when it has been made using ion beam thinning methods. Not only is the angular distribution of the beam entering the specimen changed as a function of the thickness of the contamination layer above it but so are the phases of the electrons scattered by the generally amorphous material. In previous work on the effects of contamination on AlAs|GaAs structures we have demonstrated that for hollow cone imaging the consequences can be a change in the atomic level contrast rather than simply the superposition of random noise on the image [4].

This previous work was carried out using unfiltered images and it was thus difficult to separate the effects on the image detail caused by the contributions from the increased angular spread due to elastic scattering in the contamination layer and by the subsequent elastic scattering of the electrons which had lost energy in the contamination layer. Here we attempt to separate the distinct contributions. The approach we have taken has been to compare quantitatively both a filtered and an unfiltered through focal series of (001) images of a test sample of the tetragonal block oxide, $(Nb_2O_5)_9(WO_3)_8$, ground and suspended from a holey carbon support film, in areas of each of the images where the crystal was superposed by a carbon overlayer as well as where it was not.

The microscope used was a JEOL 4000FX with a modified objective lens, designed by K. Tsuno of JEOL, with a measured $C_c$ of 1.4mm and a $C_s$ of more approximately 2mm allowing somewhat enhanced resolution relative to the normal FX versions of this microscope (transfer has been measured to extend for amorphous carbon to just less than 0.2nm) as well as the retention of an EDX analysis capability. Of equal importance, an objective mini-lens was designed by Y. Arai of JEOL to fit in the lower bore of the objective thus allowing the normal selected area apertures to be used as objective apertures for conventional bright and dark field microscopy. Since the microscope is fitted with a Gatan filter this mini-lens can also facilitate filtered imaging by allowing reduced magnifications to be used prior to the spectrometer. While the Gatan filter has excellent properties its entrance aperture at the screen level is only 3mm.

## RESULTS AND DISCUSSION

The area examined, and shown in fig. 1 at an enhanced contrast level, was obtained unfiltered and recorded digitally with full retention of the absolute intensities at a defocus of −74nm. The overfocus of the carbon support film relative to that of the oxide edge demonstrates that the carbon film is ~260nm above the oxide. Fig. 2 shows areas averaged for ~8 equivalent blocks taken from the original focal series of images at, as far as possible, equivalent thicknesses a single unit cell from the edge of the oxide. Here we show in the top two rows the unfiltered images and in the bottom two rows those obtained after filtering out energy losses above 5eV. The three rows of images were obtained at defoci of −74nm, −116nm and −158nm, the defoci being determined for the last pair of images from the amorphous layer on the edge of the oxide. We can note the reversal of contrast for the −158nm defocus images. All images have been scaled to equate the vacuum intensity to 1. Interestingly the vacuum intensity was ~20% less in the filtered than in the unfiltered images.

Before considering any changes in the *contrast* caused by differences in the relative contributions from energy loss electrons and from the change in angular spread caused by the carbon it is immediately clear that the mean *intensity* (as shown in fig. 2) is reduced with the carbon overlayer especially when filtered. From these mean intensities we can calculate the fractions scattered independently due to inelastic scattering and lost completely from the image for the oxide and the carbon as shown in table 1. This table shows that even for the very thin (~10nm) region of oxide examined ~15% of the electrons are inelastically scattered and if a carbon layer is present then this fraction rises to 28%. In addition when carbon is present about 13% of the electrons entering the sample are lost completely by processes presumably involving both elastic and inelastic scattering to high angle upper Laue zones as well as phonon scattering. A summary of the scattering processes showing their relative magnitudes is shown in fig. 3.

|  | oxide (10nm) | carbon (50nm) |  |
|---|---|---|---|
| elastically scattered | 0·43 | 0·04 | Table 1. Fractions of electrons lost |
| inelastically scattered | 0·15 | 0·15 | from the incident beam in the |
| lost completely | 0·11 | 0·02 | oxide and carbon layers |

It is simulations of type shown in fig. 4 that are normally used for comparison with images such as the "unfiltered with carbon" row in fig. 2 and the differences in the contrast levels if not in the pattern are startling. Further simulations done for a range of both smaller and larger thicknesses indicated from the effect of pattern reversals that the specimen could not have had a thickness outside the 7 to 10nm range. Greater accuracy was not attempted since, as we will see, the specimen thickness is not critical in the determination of the image/simulation mismatch.
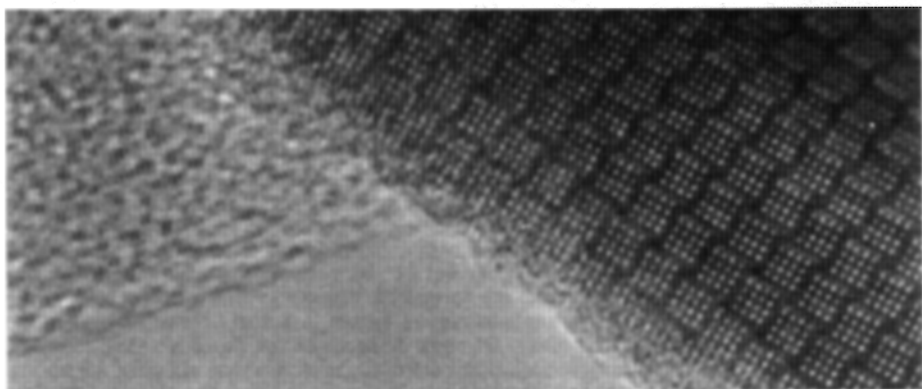


2nm ————

Fig. 1 High resolution image of $(Nb_2O_5)_9(WO_3)_8$. Black=0·71 and white=1·33 where the incident intensity=1.

| defocus | −74nm | −116nm | −158nm |
|---|---|---|---|

| | | mean intensity | | | |
|---|---|---|---|---|---|

**unfiltered**

no carbon — 0·89

with carbon — 0·88

**filtered**
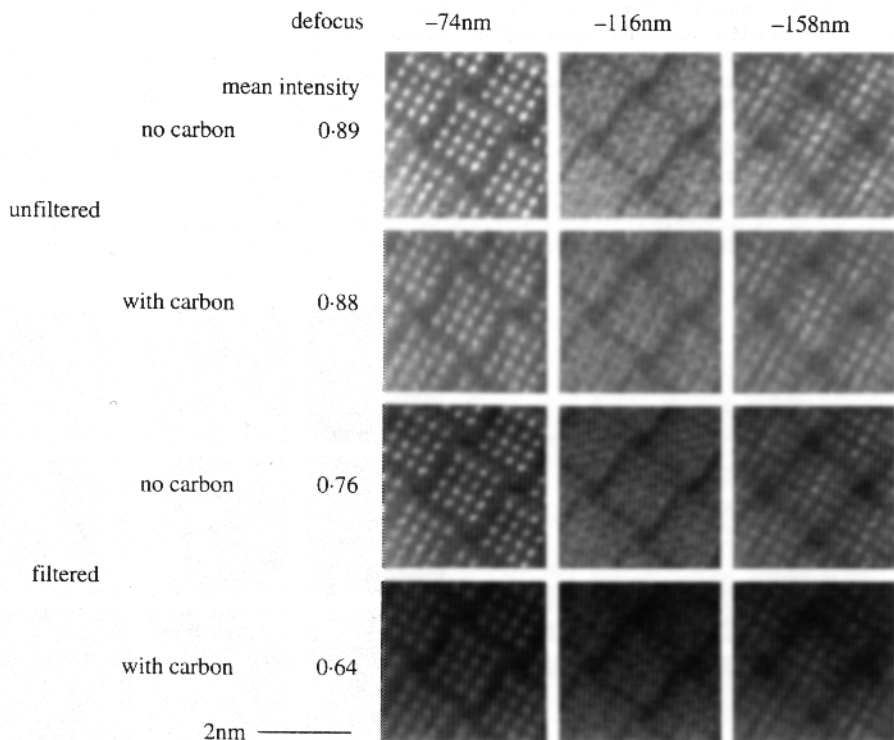
no carbon — 0·76

with carbon — 0·64

2nm ———

Fig. 2  Experimental images averaged over ~8 unit cells a single unit cell from the edge of the oxide. Black=0·3 and white=1·2.
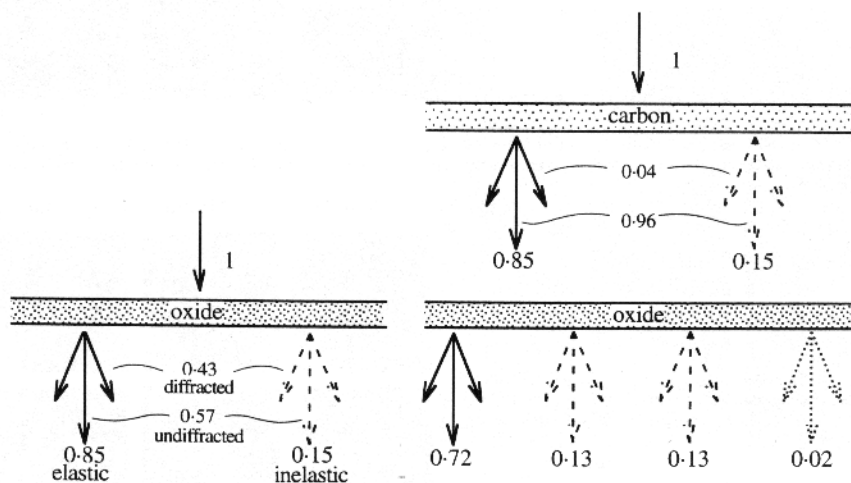
Fig. 3  Scattering processes in an oxide film without (left) and with (right) a carbon overlayer. The numbers give the fractions of the electrons scattered by each process.

We next examined the various contributions to the oxide image which should result from the known elastic (0.04) and rather greater (0.15) inelastic scattering from the carbon as well as from the inelastic scattering in the oxide of the fraction of electrons remaining elastically forward scattered after passing through the carbon (0.13). It will be remembered that only about 72% of the final image was measured to be elastic. These calculations were performed using an incoherent model where electrons that have lost energy $\Delta E$ form an image overfocus by $\Delta f = 1.28 C_c \Delta E/E$. The effect is to perform an average as a function of focus and contributions at the plasmon loss itself for carbon, at 22.5 eV, are overfocus relative to the elastic image to which they will be added by about 2 Scherzer units. This difference in focus is, for the block oxide examined, such as to cause a contrast reversal of the inelastic component of the simulation relative to the elastic component as shown in fig. 5. The mean intensity here, at 0.12, is small
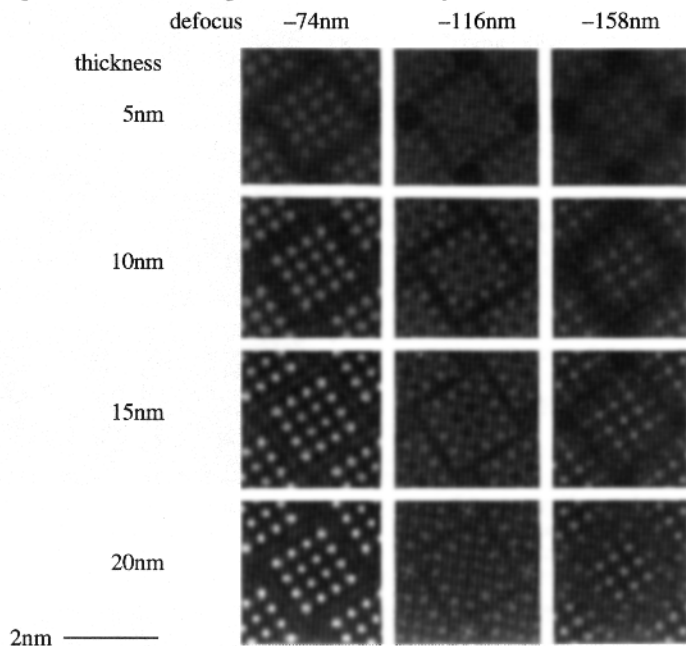


Fig. 4 Conventional elastic simulations of the oxide as a function of thickness and defocus. The microscope parameters used were $C_s$ 2mm, convergence 1mrad, focal spread 10nm and vibration 0·05nm. Black=0·3 and white=2.5.
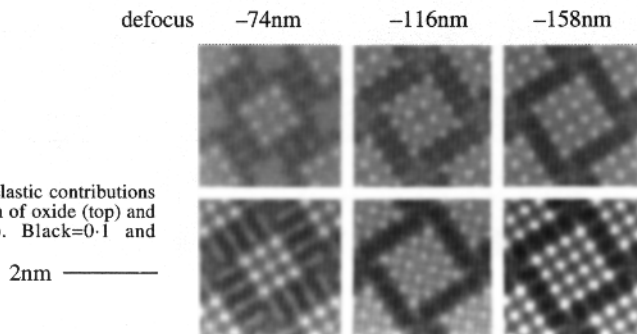


Fig. 5 Simulations of the inelastic contributions to the images caused by 10nm of oxide (top) and 50nm of carbon (bottom). Black=0·1 and white=0·2.

498

compared with that of the elastic image (1) but will nonetheless certainly change the pattern of the image as well as reduce the contrast. The contribution to the overall image due to the elastic scattering of the carbon, effectively causing a change in the convergence onto the oxide beneath it, required the simulation of the angular scattering distribution from an appropriately thick (50nm) layer (above the 10nm thick oxide), sectioned into slices occupied randomly at the atomic density (90·5 atoms/nm$^3$) of carbon, with the carbon scattering factor being modulated by the measured scattering pattern from the carbon support. While individual models gave high random phase contrast additions to the oxide image at contrast levels comparable to that seen for the oxide alone, it was found that averaging only ten such models demonstrated that the overall effect of carbon was simply to add a background at 4%, as would be expected from table 1. The lack of a contribution to the pattern of the oxide image is in contrast to the effects seen due to such scattering in hollow cone imaging [4].
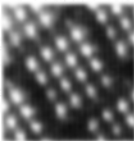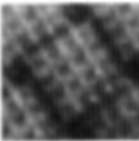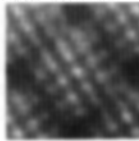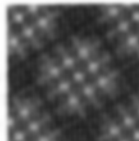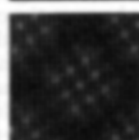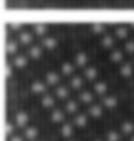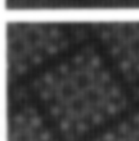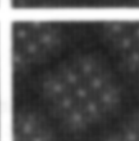
| | defocus | | −74nm | −116nm | −158nm |
|---|---|---|---|---|---|
| a) Experimental unfiltered with carbon e) with mean and contrast scaled to match next row | mean 1 | contrast 0·30 | | | |
| b) Simulated elastic | 1 | 0·30 | | | |
| c) Experimental filtered with no carbon | 0·76 | 0·11 | | | |
| d) Simulated elastic after allowing for 15% inelastic and 11% total losses | 0·76 | 0·30 | | | |
| e) Experimental unfiltered with carbon overlayer | 0·88 | 0·06 | | | |
| f) Simulated images with oxide and carbon inelastic scattering and carbon elastic scattering | 0·88 2nm —— | 0·20 | | | |

Fig. 6 Comparison of experimental and simulated images. The column "mean" is the average intensity in the image on the scale where the incident intensity is 1 and the column "contrast" is a measure of the image contrast given by the −74nm defocus image standard deviation divided by the mean.

We can now compare the various experimental and simulated images. This is done in fig. 6 where all the images and simulations are shown on the same intensity scale and with black and white levels of 0·5 and 1·8. It can be seen that the unfiltered images for the oxide with carbon layer (fig. 6e) have very low contrast (0·06) and that this is increased by nearly a factor of two to 0·11 by the removal of the effects of the 50nm carbon layer and energy filtering (fig. 6c). The simulations which would normally be compared with fig. 6c are shown in fig. 6b while those which would be obtained after allowing for the 15% inelastic and 11% total losses in the microscope are shown in fig. 6d. While the contrast ratio of c to d is 0·37, that of fig. 6e to the simulations made including all the inelastic contributions as well as the effects of the elastic scattering of the carbon (fig. 6f) is 0·3. If there were no other inelastic contributions than these considered then these ratios should be equal. That the contrast ratio is 0·2 indicates that filtering has improved the mismatch in contrast significantly but that equally there must be some further effects reducing experimental contrast. Given that most people normalise the experimental and simulated contrast levels we have treated fig. 6e in this manner as shown in fig. 6a. The match with fig. 6b, particularly near to Scherzer defocus is now fairly good but clearly artificial. We know from the above simulations that the images must contain contributions to the *pattern* from inelastic scattering at something like the 10% level. Equally the ratio of the relative scatterings of 2.7 and 5 required for an approximate match of b/c and b/e respectively indicates that some 58% of the reduction in contrast from that generally expected is due to inelastic scattering, the background elastic contrast added by the carbon being only 4%.

## CONCLUSION

We have demonstrated that 50nm of carbon adds elastically random if high intensity phase contrast which on average adds only 4% to the background. It is not this of itself which reduces the contrast by the large factor observed. We have also shown that even at a thickness of 10nm patterns in an image should be modified at the 10% level by all inelastic contributions. Furthermore while filtering is responsible for 58% of the loss in contrast relative to theory we currently have no experimental data on other possible processes for the remaining 1-58%. Further analysis will be required on the other effects, eg higher Z contaminants, phonon scattering and electron damage, though knock-on damage due to the 400kV electron beam was negligible even after a few hours of irradiation. We emphasise that we can preclude the specimen being thinner than about 7nm both because this would prevent a pattern match at all and because the energy loss data we obtained were consistent with the oxide and C thicknesses used in the simulations. The simulations were made with a specimen vibration amplitude of 0.05nm, this being consistent with the transfer functions obtained and the Debye Waller factor used (0·3) was the same as was measured by X-ray methods [5]. Similarly the scattering factors used were reliable and obtained via the Mott formula from Rez's tables of X-ray data and $f_{el}(0)$ [6]. Effects of ionicity in reducing the scattering factors are indeed possible but would not be expected to have as large an effect as has been demonstrated on the contrast as a whole.

## ACKNOWLEDGEMENTS

## REFERENCES

1. M.J. Hytch and W.M. Stobbs, Ultramicroscopy **53**, 191 (1994)
2. W.M. Stobbs and W.O. Saxton, J.Microsc. **151**, 171 (1988)
3. C.B. Boothroyd and W.M. Stobbs, Ultramocroscopy **26**, 361 (1988)
4. C.B. Boothroyd and W.M. Stobbs, Ultramocroscopy **31**, 259 (1989)
5. R.S. Roth and A.D. Wadsley, Acta Cryst. **19**, 38 (1965)
6. D. Rez and P. Rez in Proc. 51 Annual Meeting of MSA